ACKNOWLEDGMENTS

The authors would like to acknowledge Professor D. Sellmyer for contributions to parts of this work. Professor Leo Falicov and Rajendra Bhandari have made valuable contributions to interpretation of the data and Philipp Sommer and Werner Frewer have constructed parts of the apparatus.

*Work supported by Office of Naval Research and U. S. Atomic Energy Commission.

†Work above 80 kOe was performed while the authors were Guest Scientists at the Francis Bitter National Magnet Laboratory, which is supported at MIT by the National Science Foundation.

[1]D. J. Beerntsen, G. A. Spiering, and C. H. Armitage, IEEE Trans. Aerosp. **2,** 816 (1964).

[2]G. A. Spiering, E. Revolinsky, and D. J. Beerntsen, J. Phys. Chem. Solids **27,** 535 (1966).

[3]E. A. Antonova, S. A. Medvedev, and I. Yu. Shebalin, Zh. Eksp. Teor. Fiz. **57,** 329 (1969) [Sov. Phys.-JETP **30,** 181 (1970)].

[4]A. H. Thompson, R. F. Gamble, and R. F. Koehler, Jr., Phys. Rev. B **5,** 2811 (1972).

[5]R. C. Morris, R. V. Coleman, and Rajendra Bhandari, Phys. Rev. B **5,** 895 (1972).

[6]M. H. Van Maaren and G. M. Schaeffer, Phys. Lett. **20,** 131 (1966); R. Kershaw, M. Vlasse, and A. Wold, Inorg. Chem. **6,** 1599 (1967).

[7]F. R. Gamble, F. J. DiSalvo, R. A. Klemm, and T. H. Geballe, Science **168,** 568 (1970).

[8]Y. B. Kim and M. J. Stephin, in *Superconductivy,* edited by R. D. Parks (Marcel Dekker, New York, 1969), p. 1120.

[9]S. Foner, E. J. McNiff, Jr., A. H. Thompson, F. R. Gamble, T. H. Geballe, and F. J. DiSalvo, Bull. Am. Phys. Soc. **17,** 289 (1972).

[10]Alexander L. Fetter and Pierre C. Hohenberg, in Ref. 8, p. 860.

[11]W. E. Lawrence and S. Doniach, in *Proceedings of International Conference on Low Temperature Physics, 1970* (Academic Press of Japan, Tokyo, 1970), Vol. 12, p. 361.

[12]R. Bachmann, H. C. Kirsch, and T. H. Geballe, Solid State Commun. **9,** 57 (1971).

[13]M. H. Van Maaren and H. B. Harland, Phys. Lett. A**29,** 571 (1969).

[14]W. L. McMillan, Phys. Rev. **167,** 331 (1968).

[15]See, for example, J. A. Wilson and A. D. Yoffe, Adv. Phys. **18,** 193 (1969); R. B. Murray, R. A. Bromley, and A. D. Yoffe, J. Phys. C **5,** 746 (1972); R. A. Bromley, R. B. Murray, and A. D. Yoffe, J. Phys. C **5,** 759 (1972).

[16]R. Huisman, R. DeJonge, C. Hass, and F. Jellinek, J. Solid State Chem. **3,** 56 (1971).

[17]M. Marezio, P. D. Dernier, A. Menth, and G. W. Hull, Jr., J. Solid State Chem. **4,** 425 (1972).

[18]E. Ehrenfreund, A. C. Gossard, F. R. Gamble, and T. H. Geballe, J. Appl. Phys. **42,** 1491 (1971).

[19]R. A. Bromley, Phys. Rev. Lett. **29,** 357 (1972).

[20]B. T. Geilikman and V. Z. Kresin, Fiz. Tverd. Tela **5,** 3549 (1963) [Sov. Phys.-Solid State **5,** 2605 (1964)].

PHYSICAL REVIEW B VOLUME 7, NUMBER 3 1 FEBRUARY 1973

Magnetic Field Dependence of the Surface Resistance of Pure and Impure Superconducting Aluminum at Photon Energies near the Energy Gap*

W. V. Budzinski,† M. P. Garfunkel, and R. W. Markley‡
University of Pittsburgh, Pittsburgh, Pennsylvania 15213

(Received 17 July 1972)

The magnetic field dependence of the microwave absorptivity of superconducting aluminum single crystals has been determined in the frequency range 15–100 GHz, covering the spectrum near the superconducting energy gap. Measurements were made on samples of varying purity, from the purest available alumimum to aluminum doped with 3-at.% silver. In the pure case, the energy of the absorption edge was found to shift with static magnetic field by an amount of the order pv, where p is the Fermi momentum and v is the drift velocity associated with the Meissner current. The addition of impurities was found to reduce the shift in the absorption edge as expected. Furthermore, the impurities coupled with the static field to induce an unexpected effect, namely, an absorption peak near the energy of the zero-field absorption edge. The amplitude of the absorption peak was found to increase monotonically with both magnetic field and with concentration of the silver impurity. A suggestion is made that impurities and magnetic field induce a change in the BCS coherence factors (from case II to case I) which, in turn, is responsible for the absorption peak.

I. INTRODUCTION

For some years we have been making measurements of the effect of a static magnetic field on the microwave absorptivity of superconducting aluminum at photon energies $\hbar\omega$ near the energy gap 2Δ. Some of our early results have already appeared in abbreviated form[1–5] and there have been several papers dealing with the theory.[5–7] It is the purpose of this paper to present a complete account of our experiments.

The study of the microwave absorption of superconductors in a static magnetic field has consistently caused difficulties in fitting the existing theo-

ry. In the earliest experiment, Pippard[8] measured the effect of a static field on the microwave surface impedance of superconducting tin at 9.4 GHz and found a small (a few percent) change in the surface impedance which depended in a very complicated way on temperature and field. This was followed by a number of other experiments[9] on various materials at photon energies well below the energy gap (i.e., $\hbar\omega < 0.1\Delta$), which showed the small effect to be very complex, with even the sign depending on frequency, impurity level, static field strength, temperature, and relative geometry of static field, alternating field, and crystal direction. There were also a number of unsuccessful attempts at theoretical explanations[10] of these low-frequency experiments. Our technique[11] for making absorptivity measurements was well suited to extend the frequency range of the static-field dependence of the surface impedance since the superconducting sample is in the form of a disk with the absorption taking place on one of the flat faces. Thus, it is convenient to apply a static magnetic field either parallel to or normal to the alternating magnetic field and have both in the plane of the surface.

The results of our experiments on pure aluminum,[12,13] some of which have already been reported briefly,[1,2] show that the energy of the quasiparticles is modified by a $\vec{p}\cdot\vec{v}$ term, where $\vec{p}$ is the particle momentum and $\vec{v}$ is the drift velocity associated with the Meissner current. The drift velocity $\vec{v}$ is related to the vector potential $\vec{A}$ by $\vec{v} = (e/mc)\vec{A}$, where e and m are the electronic charge and mass, respectively, and c is the velocity of light. This $\vec{p}\cdot\vec{v}$ correction to the energy,[14] proposed by Budzinski and Garfunkel[1] to account for the field dependence, was then used in theoretical treatments by Maki,[15] Budzinski and Garfunkel,[2] Pincus,[6] and Garfunkel.[7] The last of these has calculated detailed curves which are in qualitative agreement with the experimental results on both aluminum[1,2,12] and zinc.[16]

The results for impure aluminum,[12,13] also partly reported in preliminary form,[3-5] are not yet quantitatively understood. It was expected that the addition of impurities, reducing the electron free path, would cause a reduction in the $\vec{p}\cdot\vec{v}$ correction because the magnitude of the average value of $\vec{p}$ (i.e., $|\langle\vec{p}\rangle|$) for a particle scattered by impurities is smaller than for an unscattered particle, as has been suggested by the Anderson theory of "dirty" superconductors.[17] We have been able to observe this effect for aluminum doped with very small amounts of silver. As the impurity level is further increased, however, a peak appears in the absorption in a static field, occurring at a photon energy equal to the superconducting energy gap. Although there are still many unanswered questions about the details, we now believe that this absorption peak may be related to a change in the coherence factors of the BCS theory[18] of absorption in superconductors.[19]

The measurements consist of determining calorimetrically the ratio of the microwave absorptivity in the superconducting state to that in the normal state at various frequencies between 15 and 100 GHz and at several values of static magnetic field up to the critical field. For good conductors, the absorptivity ratio α/α_n is indistinguishable from the surface resistance ratio $r \equiv R/R_n$, where R and R_n are the real (and X and X_n are the imaginary) parts of the surface impedance in the superconducting and normal states, respectively. The surface impedance is defined as $Z \equiv 4\pi\mathcal{E}(0)/H_{ac}(0) = R + iX$, where $\mathcal{E}(0)$ and $H_{ac}(0)$ are the amplitudes of the alternating electric and magnetic field at the surface of the sample.

II. EXPERIMENTAL TECHNIQUE

A. Apparatus

The measurements were made in essentially the same apparatus that has been described in detail by Biondi *et al.*[11] Microwaves are generated in one of a number of tunable klystrons capable of producing 10–100 mW of continuous power. The frequency is determined to about ±0.2% by means of absorption-cavity wave meters, several of which we use to cover the entire spectrum from 15 to over 100 GHz. The microwaves are then conducted through a K-band waveguide (cutoff frequency about 14 GHz) into the Dewar system and to the sample. The low temperature is maintained by a multiple-Dewar system: liquid nitrogen, liquid He^4 at about 1.1 K, and liquid He^3 at about 0.35 K. The low-temperature portion of the apparatus, shown in a simplified diagram in Fig. 1, is surrounded by liquid He^4 at about 1.1 K. Liquid He^3, in the toroidal container shown, is pumped to a temperature of about 0.35 K. The cold section is thermally isolated from the He^4 bath by having only poor thermal conductors connecting from one section to the other (thin-walled stainless steel for tubes and waveguide, and fine tinned-manganin wire for electrical connections). Outside the Dewar system, but surrounding the sample region, are a set of Helmholtz coils for canceling the geomagnetic field to less than 0.01 G and a second set of Helmholtz coils for applying a magnetic field parallel to the sample surface. For calibration of all carbon and germanium resistance thermometers marked T, the temperature is determined from the He^3-vapor-pressure–vs–temperature tables[20] using the measured pressure[21] above the liquid in the vapor-pressure bulb. The microwaves, which enter at the input waveguide, go through the mode suppressor (two plane vanes

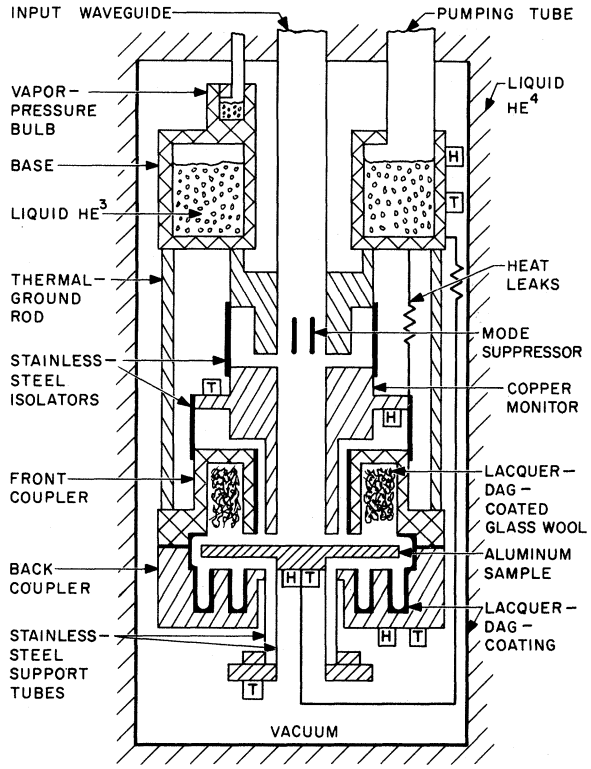

FIG. 1. Schematic diagram of the low-temperature portion of apparatus. Boxes containing *H* and *T* refer to 100-Ω manganin-wire electrical heaters and carbon (or germanium) resistance thermometers, respectively. See the text for a description of the operation of the apparatus.

across the long dimension of the waveguide) to assure that only those waveguide modes with electric field normal to the vanes are transmitted to the sample. The "copper-monitor" section of the waveguide serves to measure the incident power to correct for power-level drift. The sample, a circular disk with a diameter of about 3.0 cm and a thickness of 0.15 cm, is the electrical termination of the waveguide. The sample and copper monitor are only loosely connected to the He^3 bath through heat leaks so that energy absorbed will raise their temperatures. The coupler, however, is thermally grounded to the He^3 bath. The temperature of the base is controlled electronically using the thermometer on the base as the sensing element while power is dissipated in the heater *H* on the base to maintain the desired temperature.

The power absorbed in the sample is determined by measuring the extra power that must be dissipated in the heater on the sample to establish the same sample temperature as was established by the microwaves. This is normalized to the incident intensity by a similar measurement on the copper monitor. The other thermometers and heaters help to establish equivalent thermal patterns and to detect microwave leakage around the sample. For a somewhat more detailed description of the apparatus see Biondi *et al.*[11]

B. Sample Preparation

All samples were made from initially high-purity aluminum[22] (less than 1-ppm impurity). To obtain the desired levels of impurity, silver was added in the melt of several ingots in various quantities to obtain 0.02-, 0.2-, and 3-at.% silver impurity. These ingots, as well as the pure ingots, were then grown into single crystals (~3.2 cm diam and ~15 cm long) by cooling in a temperature gradient from the melt in graphite crucibles. For the 0.2- and 3-at.% nominal impurity an attempt was made to cool rapidly from about 500 °C by blowing cold helium gas across the crucible. Rapid cooling is necessary to prevent the silver impurity from precipitating out during slow cooldown, since at room temperature silver is not soluble in aluminum in the larger quantities. The single-crystal ingots were oriented by x-ray back-scattering techniques and a sample was cut to the desired size and shape and with the desired crystal orientation (to within about 2°) by spark machining. The front face of each sample was mechanically polished flat using a fine diamond-dust abrasive, and then chemically polished with a solution of 94% orthophosphoric acid and 6% nitric acid at 95 °C. After polishing, the samples were reannealed near the melting point, well above the temperature at which the solubility of silver is only 3 at.%. (The most impure specimens were then cooled rapidly from about 500 °C to try to maintain the high level of impurity. At any rate, we measure the residual resistance of the samples to determine the electron mean free path, which is the quantity we are interested in. The percentage of silver dissolved should be considered only as an indication of the impurity level.) The samples were then repolished chemically before mounting in the apparatus. The purer samples have a near-mirrorlike finish with a light filming and a few pock marks, while the most impure samples had a rather matte surface and the 3-at.% Ag sample was also somewhat discolored. We do not believe that the results were very sensitive to the surface quality since the two pure samples showed very similar results as did the two samples with nominal 0.2-at.% silver. (This may be because *all* the surfaces were sufficiently rough to cause diffuse scattering of electrons at the surface.)

A measure of the level of purity of the samples is the residual resistance ratio (RRR), which was determined from the rate of decay of eddy currents induced in the disk-shaped samples at room temperature and at 4.2 K. The RRR values for the

different samples are given, along with other properties of the samples, in Sec. III.

C. Measurements

The absorption measurements, taken as a function of both temperature and static magnetic field at constant frequency, involve recording the readings of the thermometers on the sample, copper monitor, coupler, and isolator with the microwave power on. Then with microwaves off, the powers absorbed in the sample and in the copper monitor are obtained from the current needed in the relevant heaters to reproduce the temperature rises that had resulted from the microwave energy absorption. In order to discount power-level drifts of the incident microwaves, the power absorbed in the sample is divided by the power absorbed in the monitor. These ratios are then normalized to the value of the same ratio measured just above the superconducting transition temperature T_c, giving the ratio of absorptivities (or the surface resistance ratio r) in the superconducting and normal states, respectively.

The absorption measurements have been used in several ways. In zero static magnetic field at a low frequency ($\lesssim 20$ GHz), careful measurements of the temperature dependence of the absorption shows a sharp break at the transition temperature T_c of the sample, as shown in Fig. 2(a). Similarly, the critical magnetic field is obtained from absorption measurements made as a function of static magnetic field, as shown in Fig. 2(b). The transition temperatures and critical magnetic fields for all of our samples were obtained in this way. For the static field measurements we chose the static field either parallel [H(parallel)] or perpendicular [H(normal)] to the alternating magnetic field H_{ac}, as shown in Fig. 3.[23]

For a detailed discussion of the sources of error of the measurements, we again refer to Biondi *et al.*[11] We note here that the temperature, frequency, and magnetic field are all determined to an accuracy well beyond that needed for our discussion. The primary source of error of the measurements is the leakage of microwaves around the sample, or otherwise out of the waveguide, getting to the back side of the sample, either on the support tube or on the thermometer and heater (see Fig. 1). We expect that this limits the accuracy of the absorption determination to about 1 at.% at most frequencies, but with errors of several (2–4) percent in the neighborhood of certain special frequencies. These errors, of course, all indicate a higher absorption than the correct one at the frequency in question. We do not expect these errors to depend appreciably on the static magnetic field. It may be noticed in the results that at the lowest frequencies and largest static magnetic field there

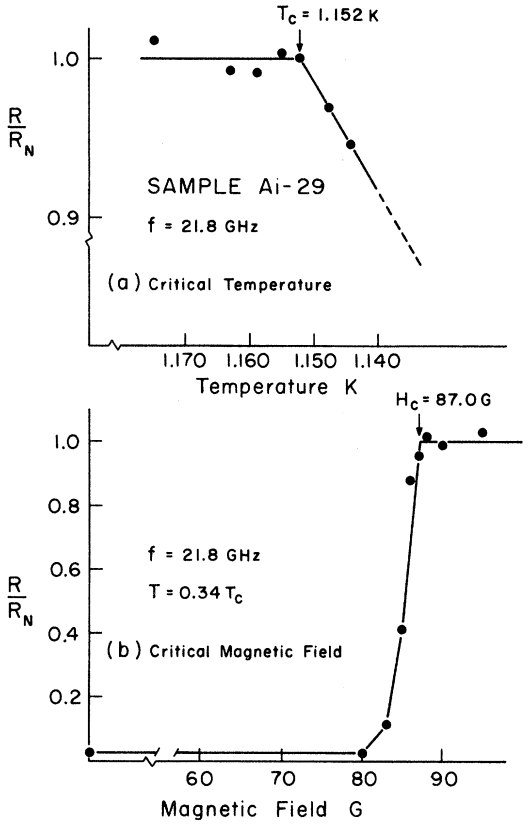

FIG. 2. (a) Low-frequency temperature dependence of the surface resistance ratio near the superconducting transition temperature. The knee of this curve occurs at the transition temperature. (b) Magnetic field dependence of the surface resistance ratio. The critical magnetic field is the value of field at the upper knee.

is an appreciable absorption. This is probably caused by the combination of two effects, namely, the edges of the sample are in the intermediate state at large field values, and there is appreciable leakage of microwaves to the edge of the sample at long wavelengths. We have discounted those points which show this inconsistency.

III. RESULTS

The field dependence of the absorption is measured by fixing the frequency and temperature while changing the static magnetic field. This method of data taking makes the differences in absorption—from one value of field to another—more accurately determined than the individual values of the absorption. The results for the six samples are displayed in Figs. 4–9, where the surface resistance ratio $r = R/R_n$ is plotted as a function of frequency at various values of the static magnetic field. From the zero-field curve in each of these figures, we derive the energy gap at approximately $T = 0.34$ K, which is then extrapolated to $T = 0$ K using the

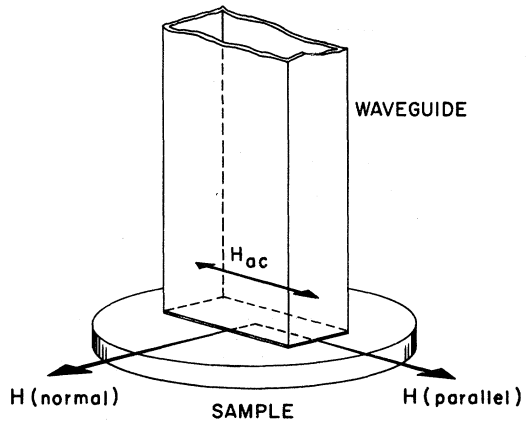

FIG. 3. Schematic diagram showing geometry of sample, static magnetic field [either H(normal) or H (parallel)], and microwave magnetic field (H_{ac}).

temperature dependence of the BCS theory. The values of the energy gap are presented in Table I along with the transition temperature, nominal impurity level, RRR, crystal orientation, and several derived properties of each sample.

There are several features of the curves that are of interest. First, we note that for the pure samples Al-18 and Al-24, shown in Figs. 4 and 5, there is a large shift in the onset of absorption.

In order to compare the effect of a static field on the two samples, we plot in Fig. 10, $\delta r \equiv r(H) - r(0)$, the change in surface resistance ratio for

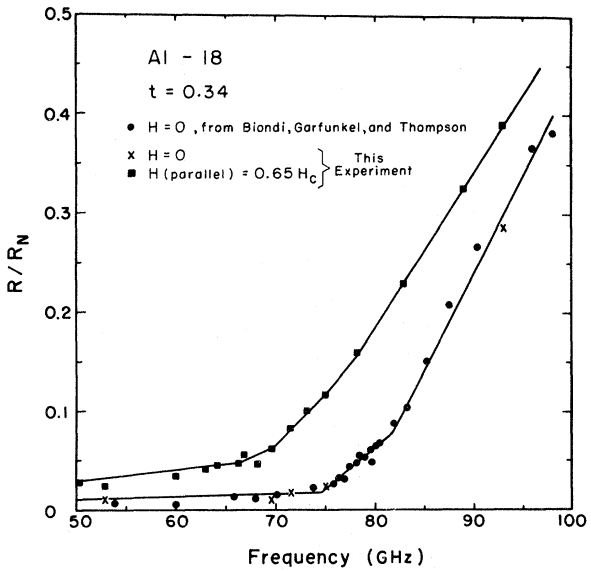

FIG. 4. Surface resistance ratio vs frequency for Al-18 (pure aluminum). The absorbing surface is a (110) crystal plane. The solid-circle data are from the work of Biondi, Garfunkel, and Thompson given in Ref. 11.

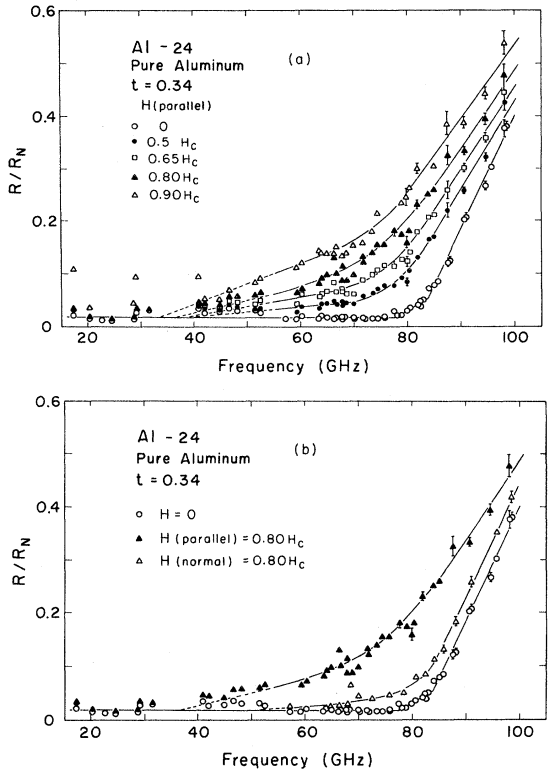

FIG. 5. Surface resistance ratio vs frequency for Al-24 (pure aluminum). The absorbing surface is a (100) crystal plane: (a) H(parallel); (b) a comparison of H(parallel) and H(normal) at $0.80H_c$.

H(parallel) = $0.65H_c$ for both samples. Clearly, at this value of field the shift in onset frequency $\delta\nu_0 \equiv \nu_g - \nu_0$ (where ν_g is the gap frequency and ν_0 is the onset frequency) is about 35 GHz. The two samples, having different crystal orientations, show essentially the same behavior in this plot, indicating that crystal orientation does not appreciably affect the static field dependence, but only has a small effect on the zero-field frequency dependence (as was seen in Biondi *et al.*[11]). Figure 11 shows plots of δr for various values of the static field for Al-24. The shift in onset frequency, $\delta\nu_0$, may be the same for both orientations of static field, but since the value for δr is smaller by at least a factor of 3 for H(normal), it is not possible to get an accurate measure of the shift for this case. From Fig. 11(a) we obtain the shift in the onset frequency $\delta\nu_0$ as a function of field, which is then plotted in Fig. 12. Although the scatter is large, it can be fitted with a linear relationship between H(parallel) and the shift in the onset frequency $\delta\nu_0$.

As can be seen in Fig. 13 for Al-29, the shift $\delta\nu_0$ for 0.02-at.% silver doping at H(parallel) = $0.65H_c$ has dropped from its value in the pure

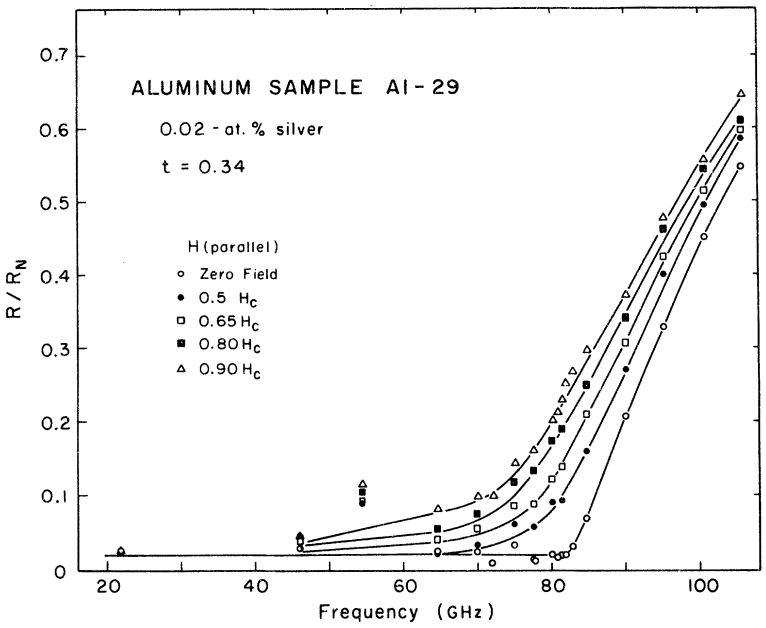

FIG. 6. Surface resistance ratio vs frequency for Al-29 (aluminum doped with 0.02-at.% silver). The absorbing surface is a (100) crystal plane and the static magnetic field is parallel to the microwave magnetic field.

samples. In fact, the decrease in $\delta\nu_0$ would be even greater if it were not for the long tail exhibited by δr as it approaches ν_0 from above. This is in agreement with the expectation that the $\vec{p}\cdot\vec{v}$ correction is reduced when scattering reduces the effective magnitude of $\vec{p}$ for most electrons, while the tailing comes from those few electrons that are unscattered. The reduction in $\delta\nu_0$ is seen to continue for the 0.2-at.% silver–doped sample Al-26, shown in Fig. 14, although the onset frequency is obscured by the occurrence of the "resonance" absorption peak that has appeared clearly in Figs. 7 and 8 for these levels of impurity. As we go to our most impure sample, Al-3000 in Fig. 9, the shift $\delta\nu_0$ has become obscured because the large absorption peak dominates the frequency region near the energy gap.

The most notable feature of the three dirtiest samples is the absorption peak that occurs close to the zero-field absorption edge. Furthermore, if one examines Fig. 6, the curve for Al-29, there is even in this relatively pure sample some evidence of an absorption peak for the largest field values near the zero-field onset frequency of about 82 GHz. It appears that the combination of static magnetic field and short electron free path generate the absorption peak as the most noticeable feature for H(parallel). However, as we note in Fig. 7(b), the H(normal) curve for Al-26, there is no evidence of an absorption peak. The appearance of the peak is thus seen to be a characteristic of H(parallel) and not of H(normal).

The existence of the absorption peak is the most puzzling aspect of these results, and although a possible origin of the peak will be mentioned later in this paper and discussed at length in a subsequent paper,[19] we are not at all confident that we have made the correct identification. For this reason

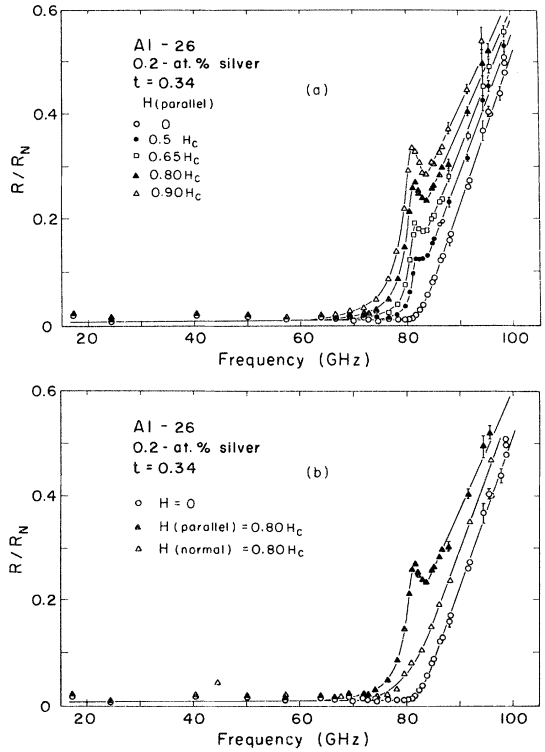

FIG. 7. Surface resistance ratio vs frequency for Al-26 (aluminum doped with 0.20-at.% silver). The absorbing surface is a (100) crystal plane: (a) H(parallel); (b) a comparison of H(parallel) and H(normal) at $0.80H_c$.

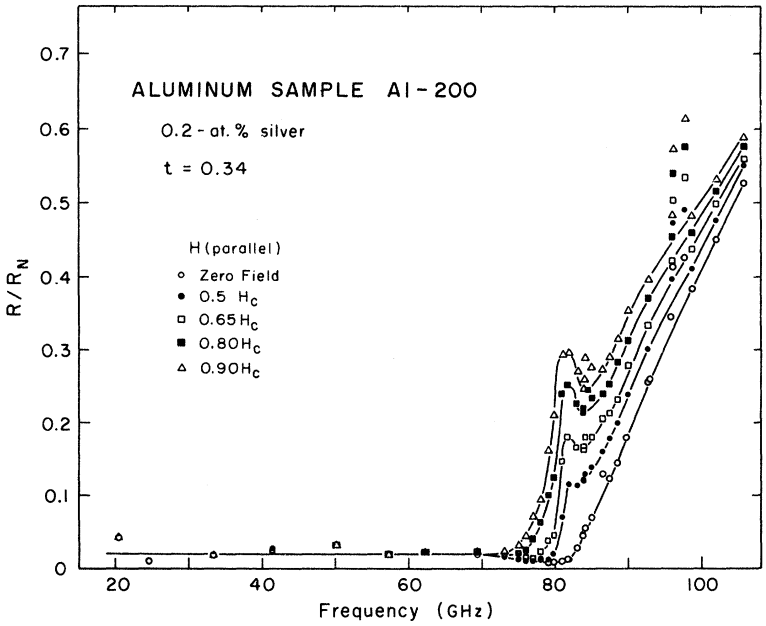

FIG. 8. Surface resistance ratio vs frequency for Al-200 (aluminum doped with 0.20-at.% silver). The absorbing surface is a (100) crystal plane and the static magnetic field is parallel to the microwave magnetic field.

we present the data in several different ways, hoping to shed some additional light on the problem.

First, in order to display the peak itself we subtract from the H(parallel) data of Al-29, Al-200, and Al-3000 a smooth curve having the same shape as the zero-field curve for each, but shifted in frequency to give a nearly symmetric bell-shaped difference curve. These three are displayed in Figs. 15(a)–(c) where the growth of the absorption peak with impurity is clearly evident. From the curves of Fig. 15, it is simple to construct the dependence of peak amplitude on magnetic field and on impurity level. These derived curves are shown in Figs. 16 and 17, respectively. The field dependence (Fig. 16) is shown for each of the three samples and fitted by a straight line—the scatter is too great to say any more than that the results are consistent with a straight-line dependence. By extrapolating each of the curves of Fig. 16 to $H/H_c = 1$, and by plotting that peak amplitude against the reciprocal of the electron mean free path l in Fig. 17, we obtain a reasonably good straight line. This suggests that the peak height is directly proportional to $(H/H_c)/l$ for all silver-doped samples, although

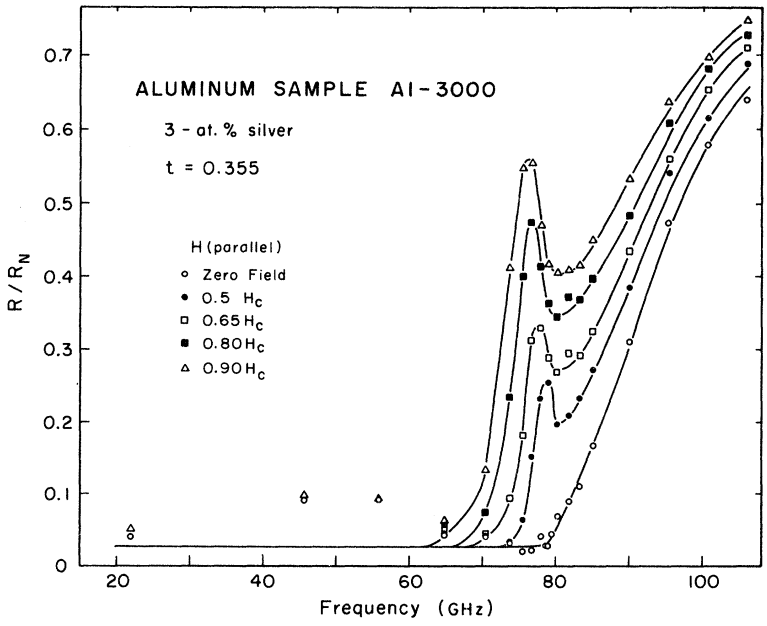

FIG. 9. Surface resistance ratio vs frequency for Al-3000 (aluminum doped with 3.0-at.% silver). The absorbing surface is a (100) crystal face, and the static magnetic field is parallel to the microwave magnetic field.

TABLE I. Properties of the samples and comparison of the energy gap at $T=0$ K with the BCS theory (Ref. 18).

Sample	Nominal silver impurity concentration (in at.%)	Crystal direction of surface	RRR	Superconducting transition temperature (K)	Electron free path (cm)	Minimum superconducting energy-gap freq. (GHz)	$\frac{2\Delta}{kT_c}$	κ
Al-18	0.00[a]	[110]	2200	1.175 ± 0.003	3.5×10^{-3}	74.4 ± 0.5	3.04	0.010
Al-24	0.00[a]	[100]	2600	1.175 ± 0.003	4.2×10^{-3}	77.6 ± 0.5	3.17	0.010
Al-29	0.02	[100]	92	1.152 ± 0.003	1.5×10^{-4}	82.0 ± 0.5	3.42	0.019
Al-26	0.20	[100]	14.3	1.121 ± 0.003	2.2×10^{-5}	81.4 ± 0.5	3.48	0.070
Al-200	0.20	[100]	12.3	1.117 ± 0.003	2.0×10^{-5}	82.0 ± 0.5	3.53	0.075
Al-3000	3.0	[100]	5.3	1.072 ± 0.003	0.86×10^{-5}	78.8 ± 0.5	3.53	0.17
BCS							3.53	

[a]Made from 99.9999% pure aluminum ingot.

the scatter would make it just as good a fit to use the coherence length ξ in place of the electron free path l.

In Figs. 7–9 and 15, it can be noticed that as the field is increased, the absorption peak moves to slightly lower frequencies. Although this is a small effect, amounting to only 5% in the most extreme case, it appears to be clearly quadratic in field, and to be greatest for the most impure sample Al-3000. In Fig. 18, we show $\delta\nu_p \equiv \nu_s - \nu_p$, where ν_p is the frequency at the absorption peak, as a function of $(H/H_c)^2$ for Al-200 and Al-3000.

For the pure samples plotted in Figs. 10 and 11, the shift in onset frequency was found to have a linear dependence on H/H_c (within experimental accuracy) as can be seen in Fig. 12 for Al-24. If we try the same plot with the dirtier samples Al-29, Al-26, Al-200, and Al-3000, we observe that the linear relationship no longer gives a reasonable fit, but that the shift, $\delta\nu_0 = \nu_s - \nu_0$, is more nearly quadratic in H/H_c. For the purest of these, Al-29 (0.02-at.% Ag), the onset frequency is very difficult to establish because there is a long tail (see Fig. 13), and the question of whether the shift is linear or more rapid cannot be settled from these data. Nevertheless, the addition of small amounts of impurity clearly reduces the shift $\delta\nu_0$, continuing to do so until the wings of the resonance dominate the onset frequency ν_0.

IV. DISCUSSION

A. Changes in Superconducting Properties with Impurity in Zero Magnetic Field

In Table I we note that the superconducting transition temperature changes monatonically with electron free path, the highest transition temperature corresponding to the purest aluminum, in good agreement with results obtained by Chanin *et al.*[24] on the same materials. Our most impure sample,

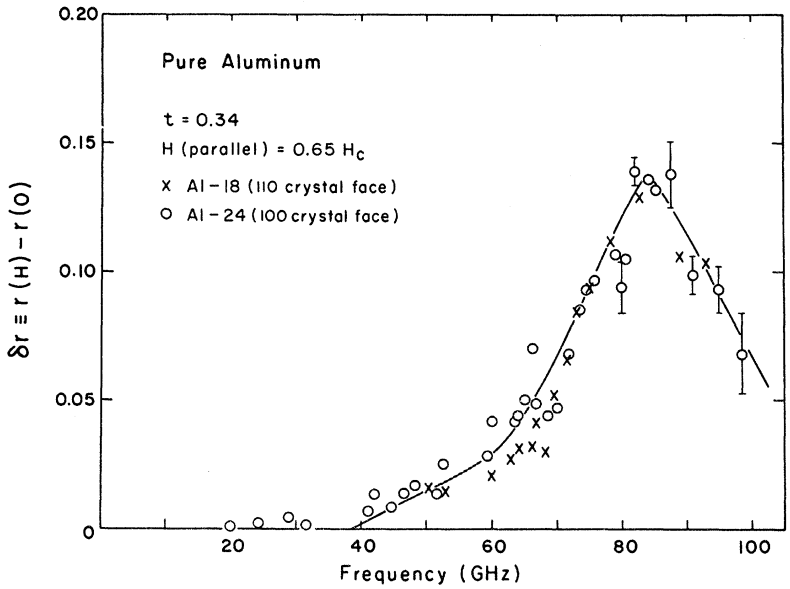

FIG. 10. Change in surface resistance ratio at H(parallel) $= 0.65 H_c$. Comparison of pure aluminum samples Al-18 and Al-24.

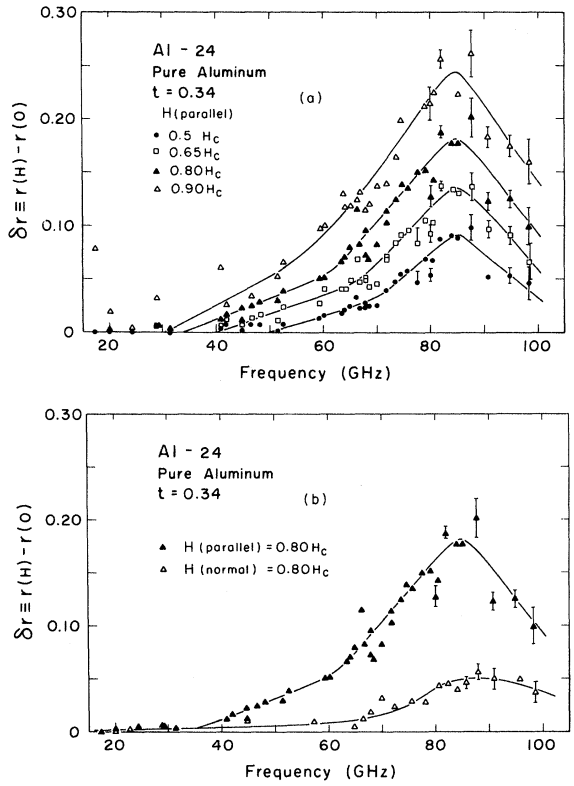

FIG. 11. Change in surface resistance ratio for pure aluminum sample Al-24: (a) various values of H(parallel); (b) comparison of H(parallel) and H(normal) at $0.80H_c$.

Al-3000, however, has a slightly lower transition temperature than would have been predicted by the extrapolation of their data.[24] Again referring to Table I, we note that the energy gap[25] increases with the addition of small amounts of impurity but finally decreases for our most impure sample, Al-3000. This is consistent with the Anderson theory of dirty superconductors,[17] in which the effect of impurities is to reduce electron free path by scattering, destroying the usefulness of the direction of the electron wave vector $\vec{k}$ as a good quantum number. The result is that the anisotropy of the energy gap is destroyed, increasing the minimum energy gap towards the mean value, and decreasing the maximum gap, which in turn decreases the superconducting transition temperature. As the anisotropy is destroyed with increasing impurity, the ratio of energy gap to transition temperature should approach the BCS[18] value ($2\Delta/kT_c = 3.53$).[26] From the column $2\Delta/kT_c$ in Table I we see that the dirtiest samples have attained this value.

B. Effects of Static Magnetic Field on Surface Resistance of Pure Superconducting Aluminum

The data for the two pure samples Al-18 and Al-24 displayed in Figs. 4, 5, and 10–12 show a large shift in the onset of absorption with static magnetic field. When these shifts were initially observed,[1,2] it was proposed that they were caused by the one-particle energy shifts associated with the Meissner currents flowing near the surface of the sample. The one-particle energy shift is given by $\vec{p}\cdot\vec{v}$, where $\vec{p}$ is the electron momentum (near the Fermi surface for all electrons of interest) and $\vec{v}$ is the electron drift velocity.

On the basis of this model for the energy shift, Pincus[6] developed a theory which introduced a $\vec{p}\cdot\vec{v}$ square-well potential for a distance equal to the superconducting penetration depth λ from the surface. He was then able to show (using as the boundary condition, specular reflection of electrons at the sample surface) that there are particular surface states that exist in the static magnetic field that permit absorption at energies as much as $|\vec{p}||\vec{v}| = pv$ below the superconducting energy gap. Unfortunately, to calculate the actual frequency-dependent surface resistance using the Pincus model[6] is both difficult and tedious, and for these reasons has not been done. It would be very in-

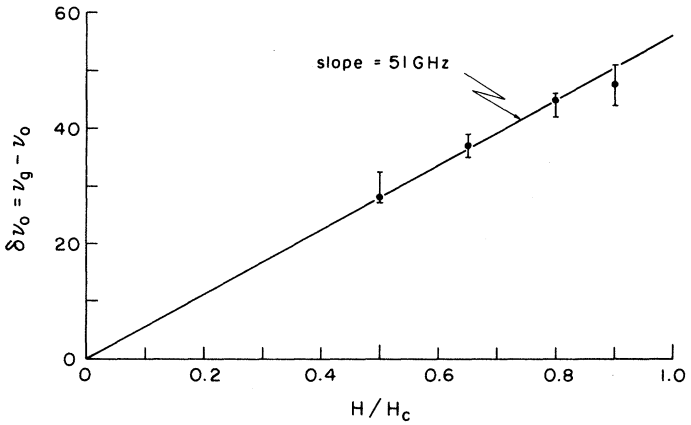

FIG. 12. Shift in onset frequency vs static magnetic field, H(parallel), for pure aluminum sample Al-24.

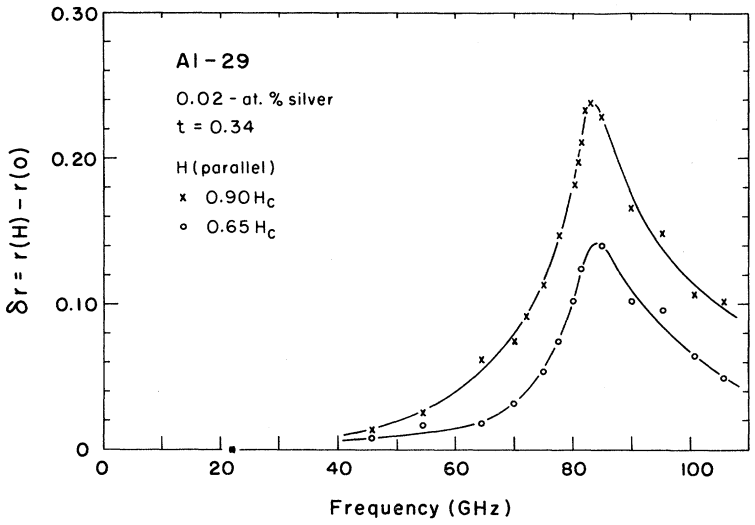

FIG. 13. Change in surface resistance ratio for Al-29 (0.02-at. % silver) for H(parallel).

teresting to see if the specular reflection boundary condition can actually account for as much absorption as is observed.

In a semiclassical approach, Garfunkel[7] used the $\vec{p}\cdot\vec{v}$ energy correction to modify the BCS[18] expressions for the bulk conductivity ratio[27] σ/σ_n, where $\sigma = \sigma_1 - i\sigma_2$ is the complex conductivity in the superconducting state and σ_n is the normal-state conductivity. The surface impedance ratio Z/Z_n in the extreme anomalous limit is then given by[27]

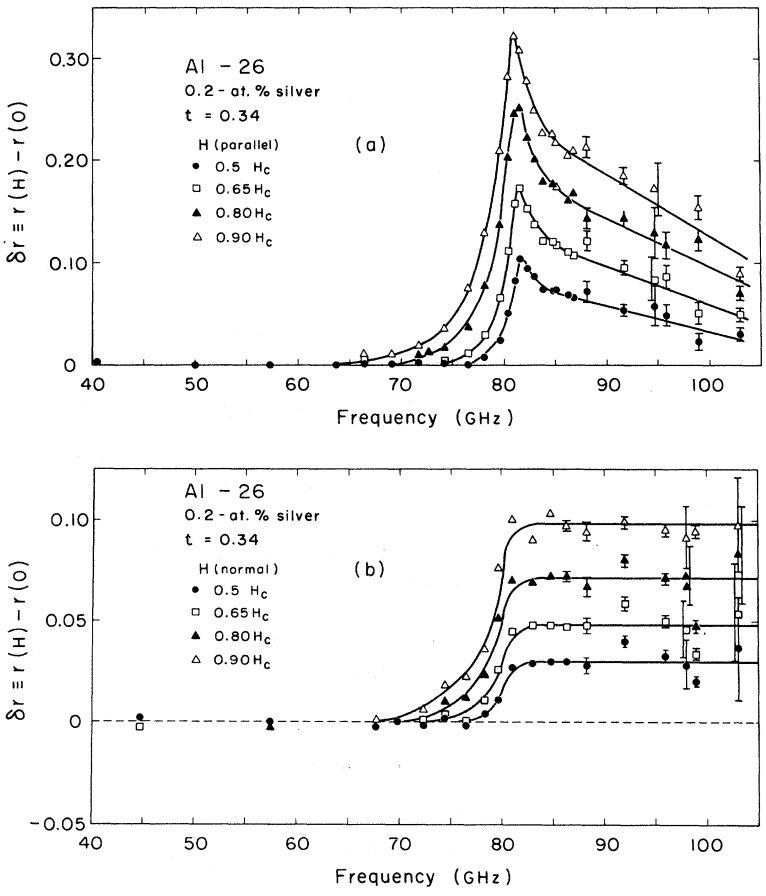

FIG. 14. Change in surface resistance ratio for Al-26 (0.2-at. % silver): (a) H(parallel); (b) H(normal).

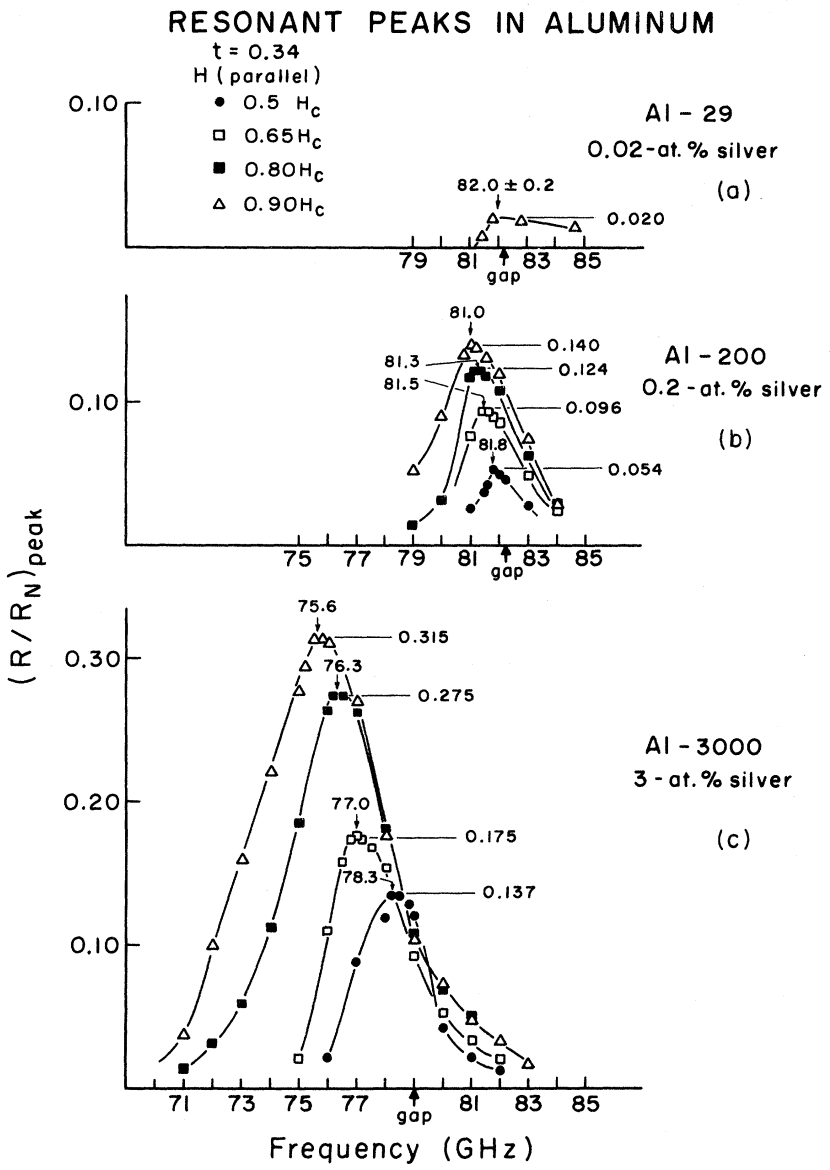

FIG. 15. Absorption peaks from surface resistance ratios for impure aluminum. These curves represent the "excess" absorption over that expected from the simple Mattis–Bardeen theory (Ref. 27). (See the text for the method of deducing these curves from the data.) (a) Al-29 (0.02-at. % silver); (b) Al-200 (0.2-at. % silver); (c) Al-3000 (3.0-at. % silver).

$$Z/Z_n = (\sigma/\sigma_n)^{-1/3} . \tag{1}$$

Pure aluminum is sufficiently close to the extreme anomalous limit (i. e., the penetration depth λ is much smaller than the superconducting coherence length ξ) for this to be an adequate approximation. In order to complete the model, Garfunkel[7] used a modification of the Pippard ineffectiveness concept[28] and the boundary condition of diffuse scattering of electrons at the surface. The boundary condition is an essential part of this model. If specular reflection were assumed, the results would be very different, yielding no shift in the onset frequency $\delta\nu_0$. The result of the above modifications is to change the BCS expressions[27] for σ_1/σ_n and σ_2/σ_n at $T=0$ K to the form[7]

$$\frac{\sigma_1}{\sigma_n} = \frac{2}{\pi\hbar\omega}\int_0^{\theta_0} \cos^2(\beta+\theta) \times \int_{\Delta-\hbar\omega-pv\cos\theta}^{\Delta} \left(1+\frac{\Delta^2}{EE'}\right)[\rho(E)\rho(E')]\,dE\,d\theta \tag{2}$$

and

$$\frac{\sigma_2}{\sigma_n} = i\,\frac{2}{\pi\hbar\omega}\int_0^{\theta_0} \cos^2(\beta+\theta) \times \int_{\Delta-\hbar\omega-pv\cos\theta}^{\Delta} \left(1+\frac{\Delta^2}{EE'}\right)[\rho(E)\rho(E')]\,dE\,d\theta , \tag{3}$$

where $E' \equiv E + pv\cos\theta + \hbar\omega$, $\rho(E) = E/(E^2-\Delta^2)^{1/2}$ is the BCS density of states, β is the angle between the static and alternating magnetic fields, θ is the

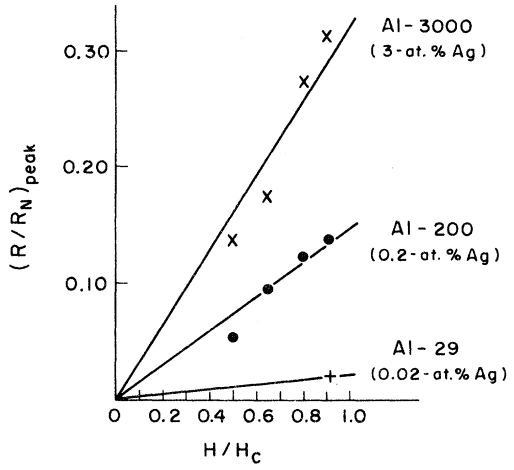

FIG. 16. Absorption peak height vs static magnetic field for impure aluminum.

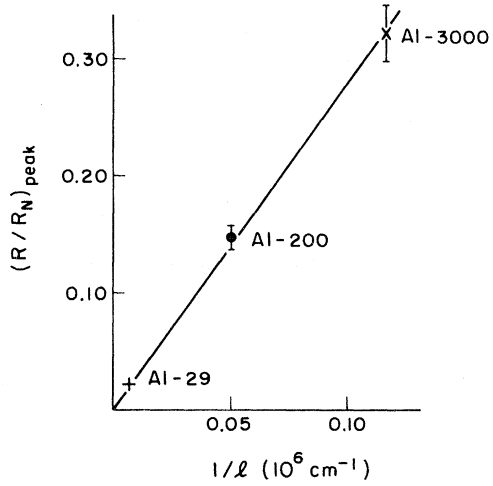

FIG. 17. Absorption peak height vs reciprocal electron free path in aluminum.

angle between p and v, and θ_0 is defined by $\cos\theta_0 = (2\Delta - \hbar\omega)/pv$. Using Eqs. (2) and (3) it is necessary to have a relationship between the static magnetic field H and the product pv. Garfunkel[7] defined a quantity H_0 which is that value of magnetic field for which $pv = \Delta$. His results are given in terms of $h_0 \equiv H/H_0$, a reduced magnetic field. Since H_0 is defined in terms of the microscopic parameters p and Δ, and is sensitive to the approximations of the model, we do not expect to be able to accurately evaluate it in terms of the actual critical magnetic field. If, however, one were to take the model seriously and use an appropriate estimate for p,[29] one finds that at $T = 0$ K, $\alpha_{th} = (H_0/H_c)_{th} \approx 1.9$ (where the subscript th means that α is a theoretical estimate[29]). We will, however, treat the constant α as a parameter to be determined from the experiment.

Equations (2) and (3) have been evaluated by Garfunkel[7] and the surface impedance calculated from Eq. (1). In Fig. 18 we display his results for H(parallel). For comparison of theory with experimental results, we find from Fig. 12 $\alpha_{expt} = \nu_g/2(\delta\nu_0)_{H=H_c} \approx 0.76$ (where the subscript expt means that the value is obtained from the data of this work), and calculate the change in the surface resistance ratio to compare with the experimental data of Al-24. However, the energy gap in the pure material is known to have anisotropy and this strongly affects the resulting fit. It therefore seemed better to evaluate α_{expt} directly from the

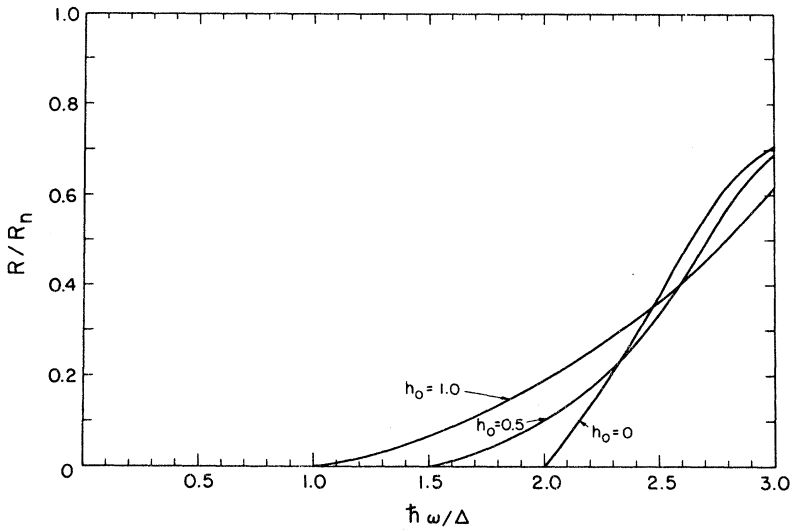

FIG. 18. Theoretical surface resistance ratios for pure aluminum in a parallel static magnetic field. The three curves are for different values of $h_0 = H/H_0$.

data. For a comparison of experiment and theory we choose the $h = H/H_c = 0.9$ curve of Fig. 11(a). To fit this curve we choose $h_0 = H/H_0 = 1.25$ corresponding to $\alpha_{expt} \approx 0.72$ (not very different from the value above). The resulting theoretical curve is shown with the experimental data in Fig. 19. The theory is for $T = 0$ K, while the experimental data are for $T = 0.34T_c$. This should be adequate since the part of the absorption from thermal excitation is smaller than the experimental error in the data. The agreement is quite good, even allowing for the one adjustable parameter α. The effect of the anisotropy of the energy gap would be to widen the main peak in the curve. The anisotropy of the energy gap of this sample was shown[11] to be 10% or greater, which would bring the theory and experiment into closer agreement than shown in Fig. 20. This agreement for aluminum along with the previously observed agreement between theory and experiment for pure zinc[16] gives some confidence in the essential correctness of the theory in this frequency region.

There are several other experiments that are related to the present experiment through the theory.[7] Maldonado and Koch[30] have measured the static field dependence of the microwave absorption at low frequencies ($\hbar\omega < \Delta$) in superconducting indium. They found that they could obtain the main features of their results using the temperature-dependent theory of Garfunkel,[7] although they had to correct an error in his temperature dependence of λ, the superconducting penetration depth. His model also predicts the temperature variation of the field dependence of the superconducting penetration depth. Measurements by Behroozi and Garfunkel[31] on aluminum give detailed agreement with the theory[7] using essentially the same value for the proportionality constant α as found in the present experiment. Finally, a series of measurements in the low-frequency microwave region ($\hbar\omega < \Delta$) made on superconducting aluminum by Raynes[32] to explicitly test a number of features of the Garfunkel theory[7] shows reasonable agreement with the theory, with some important disagreements. The disagreements are presumably a consequence of the simplifications made in the theory.

C. Effect of Impurities on Field Dependence of Surface Resistance

The addition of the silver impurity has a number of different effects which must be examined carefully to see which are significant. When discussing the pure aluminum samples it was stated that the extreme anomalous limit is an adequate approximation for both normal and superconducting states since $\lambda \ll \xi$ and the skin depth $\delta \ll l$. As impurities are added, ξ and l decrease, while λ and δ increase. For our most impure sample, Al-3000, however, we have $\lambda \lesssim \xi$ and $\delta \lesssim l$, which takes us to the range intermediate between anomalous and classical. This intermediate region has been treated by Miller[33] and by Ginsberg,[34] and shows in the zero-field case a steeper rise in absorption with frequency above the gap than either the classical or anomalous limit. Since our zero-field data for the dirty samples show this same behavior, it is evident that we are in this intermediate domain. However, since $\kappa \equiv \lambda/\xi$ is at most 0.17 for the dirtiest sample (see Table I) the samples are all type I and tend to be closer to the anomalous region than the classical region. At any rate, we assume that the important general features of the

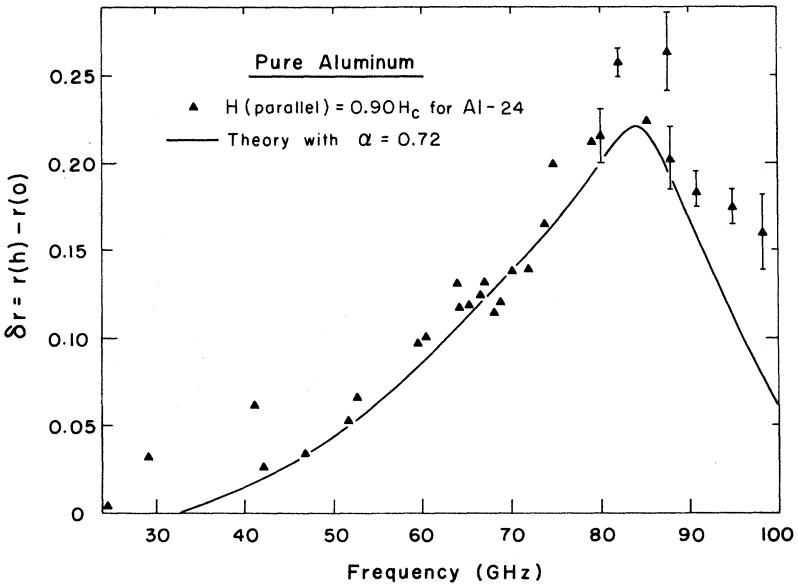

FIG. 19. Change in surface resistance ratio at H(parallel) $= 0.90H_c$. Comparison of theory and experiment for $\alpha \equiv H_0/H_c \approx 0.72$. See text for selection of α and discussion of agreement.

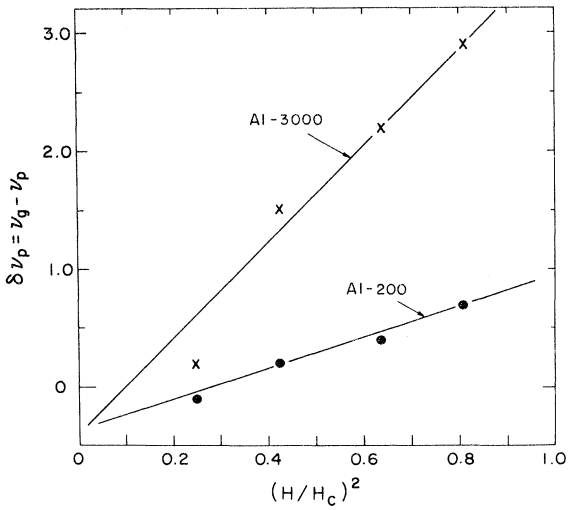

FIG. 20. Shift in absorption-peak frequency vs $(H/H_c)^2$ for Al-200 and Al-3000. The nonzero intercept at $(H/H_c)^2 = 0$ suggests that we have not selected the correct value for ν_g, but the error is too small to be significant.

results do not depend on which domain we assume and will be more or less the same in any of the limits. Only if we are interested in the absolute magnitude of the surface resistance ratio, or its rate of rise with frequency above the gap, must we concern ourselves with the details of the domain. However, in one aspect the question of how well the absorption is represented by the anomalous skin effect has some significance. That is, the "ineffectiveness concept" as used by Garfunkel[7] is valid only in the anomalous region in the superconducting state. As the penetration depth approaches the coherence length ($\lambda \sim \xi$), more and more of the electrons become effective and the approximations made by Garfunkel[7] become less and less valid. Nevertheless, we do not believe that these effects are related to either the impurity dependence of the shift in onset frequency with field, or to the appearance of the absorption peak in the impure samples.

The effect of the impurities that we believe to be most significant is the change in the nature of the one-particle electron states that was first suggested by Anderson.[17] For the pure material, the free-particle momentum ($\vec{p} = \hbar\vec{k}$, where $\vec{k}$ is the free-particle wave vector) is an adequate quantity with which to describe the state of the particle. For a spherical model of the Fermi surface, $\vec{p}$ is a vector of constant length p, and thus the energy change $\vec{p}\cdot\vec{v}$ has a value in the range $-pv$ to $+pv$ for the electrons around the Fermi surface. As we add impurities, this situation begins to change because the scattering brings electrons with two or more parts of their trajectory (each piece described by a different momentum $\hbar\vec{k}$ on the Fermi surface) into the "effective" region. That is, it is no longer possible to describe the particle state by a single plane wave (or even wave packet with most momenta near a plane-wave state). Rather one must make various combinations of these plane-wave states coming from widely different parts of the Fermi surface. For calculating the change in energy in the Meissner current, the $\vec{p}$ in the $\vec{p}\cdot\vec{v}$ term must be replaced by an average value taken over the various pieces of the particle trajectory that are in the effective zone, i.e., $\vec{p} \to \langle\vec{p}\rangle$. Clearly, as we add impurities so that there are more and more scatterings, the magnitude of $\langle\vec{p}\rangle$ (i.e., $|\langle\vec{p}\rangle|$) becomes smaller and smaller. The result to be expected is that the shift $\delta\nu_0$ is smaller for impure samples than for pure ones. Clearly the sequence of samples from pure to 0.20-at.%-Ag impurity shows this progression. For the most impure sample, Al-3000, which has 3.0-at.%-Ag impurity, the shift in onset frequency, $\delta\nu_0 = |\langle p\rangle| v/2\pi\hbar$, is masked by the absorption resonance, which although centered near ν_g has a width of several percent. At least qualitatively, then, the reduction in $\delta\nu_0$ with increasing impurity level can be ascribed to the reduction in effective electron momentum when electron scattering is introduced. This is, of course, a direct confirmation of the Anderson theory.[17]

We now come to a discussion of the absorption peak that appears for the most impure samples Al-3000 in Fig. 9, Al-200 in Fig. 8, Al-26 in Fig. 7, and even in Al-29 which shows a hint of the resonance at 82 GHz in Fig. 6. If one looks at Figs. 7–9, the resonance peak appears to be at the frequency of the zero-field gap. A more careful examination (observe Fig. 15) shows that there is a small shift with static field for the 0.20-at.%-Ag sample and a somewhat larger shift for the 3-at.%-Ag sample. These are shown to be proportional to H^2 in Fig. 20. If we assume that the peak occurs at the superconducting energy-gap frequency ν_g, then the shift indicates that the energy gap is a function of the static magnetic field. This is a known result of the Ginzburg–Landau theory[35] for materials with $\kappa > 0$. In fact, for the special case of $0 < \kappa \ll 1$ and $l > \xi_0$, Caroli[36] gives the following expression for the field dependence of the energy gap:

$$\Delta(h) = \Delta(0)(1 - \kappa h^2/4\sqrt{2}) . \quad (4)$$

If we use the value of κ for Al-200 and Al-3000 from Table I to calculate the peaks, we get only about one-half the shift shown in Fig. 20. It may be that our method of data reduction to produce Fig. 15 overemphasizes the shift, or that Eq. (4) is no longer valid for our dirtiest samples where $\xi_0 > l$.

Finally, the problem remains as to the origin of the absorption peak. We noted that in the BCS

theory[18] there were two cases considered for absorption processes. The difference in the two cases is in the coherence factor, which in Eqs. (2) and (3) is the first factor in the integral over E, namely, $1+\Delta^2/EE'$. This is the case-II coherence factor of BCS.[18] For case I, the sign is changed to $1-\Delta^2/EE'$. Case I is applicable to acoustic attenuation, while case II is applicable to electromagnetic absorption. As shown in Fig. 21 for case II, the real part of the conductivity starts slowly from zero as the frequency is increased through the gap frequency. Case I, however, has a discontinuous jump in the real part of the conductivity at the gap frequency. This led Garfunkel and Markley[5] to propose such a change to account for the absorption peaks.

In a subsequent paper,[19] the change in coherence factors for electromagnetic absorption in dirty superconductors in a static magnetic field will be discussed in more detail and some calculations show that with this change it is possible to generate an absorption peak that disappears for H(normal), as in our results. However, the justification for the change is still somewhat uncertain, and there may be, in fact, other possibilities for such an absorption peak.

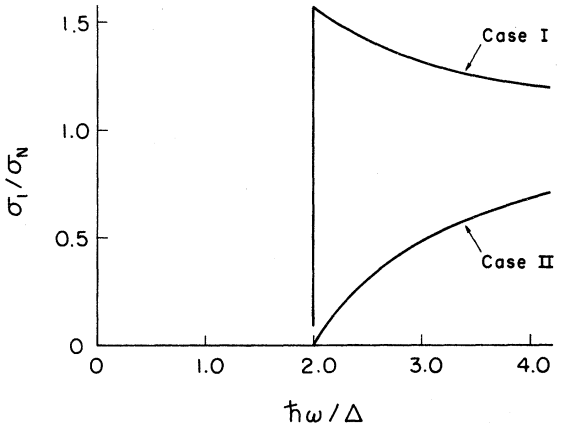

FIG. 21. Effect of coherence factor on real part of conductivity ratio σ_1/σ_n in BCS theory (Ref. 18).

ACKNOWLEDGMENTS

The authors are pleased to acknowledge many valuable discussions about this work with Richard More and Garth Wilkinson.

*Work supported by the National Science Foundation.

†Present address: Department of Physics, St. Bonaventure University, St. Bonaventure, N. Y. 14778.

‡Present address: Department of Physics, Geneva College, Beaver Falls, Pa. 15010.

[1]W. V. Budzinski and M. P. Garfunkel, in *Proceedings of the Ninth International Conference on Low Temperature Physics, Columbus, Ohio*, edited by J. G. Daunt *et al.* (Plenum, New York, 1965), Pt. A, p. 391.

[2]W. V. Budzinski and M. P. Garfunkel, Phys. Rev. Letters 16, 1100 (1966).

[3]W. V. Budzinski and M. P. Garfunkel, Phys. Rev. Letters 17, 24 (1966).

[4]W. V. Budzinski and M. P. Garfunkel, in *Proceedings of the Tenth International Conference on Low Temperature Physics, Moscow*, 1966 (Proizvodstrenno-Izdatel'skii Kombinat, Viniti, Moscow, 1967).

[5]M. P. Garfunkel and R. W. Markley, in *Proceedings of the Twelfth International Conference on Low Temperature Physics, Kyoto, Japan*, 1970, edited by E. Kanda (Keigaku Publishing, Tokyo, 1971), p. 287.

[6]P. Pincus, Phys. Rev. 158, 346 (1967).

[7]M. P. Garfunkel, Phys. Rev. 173, 516 (1968).

[8]A. B. Pippard, Proc. Roy. Soc. (London) A203, 210 (1950).

[9]Some of the other experiments for photon energies $\hbar\omega<0.1\Delta$ before 1968 follow: M. Spiewak, Phys. Rev. 113, 1479 (1959); Y. V. Sharvin and V. F. Gantmakher, Zh. Eksperim. i Teor. Fiz. 39, 1242 (1960) [Sov. Phys. JETP 12, 866 (1961)]; P. L. Richards, Phys. Rev. 126, 912 (1962); R. A. Connell, *ibid.* 129, 1952 (1963); R. T. Lewis, *ibid.* 134, A1 (1964); Yi-Han Kao and J. I. Budnick, Phys. Letters 17, 218 (1965); R. Glosser, Phys. Rev. 156, 500 (1967); and J. F. Koch and C. C. Kuo, *ibid.* 164, 618 (1967) (see Ref. 7 for other references).

[10]See, for example, J. Bardeen, Phys. Rev. 94, 554 (1954); G. Dresselhaus and M. R. Dresselhaus, *ibid.* 118, 77 (1960).

[11]M. A. Biondi, M. P. Garfunkel, and W. A. Thompson, Phys. Rev. 136, A1471 (1964).

[12]W. V. Budzinski, Ph.D. thesis (University of Pittsburgh, 1967) (unpublished).

[13]R. W. Markley, Ph.D. thesis (University of Pittsburgh, 1970) (unpublished).

[14]The modification of the quasiparticle energy by $\vec{p}\cdot\vec{v}$ has been discussed in somewhat different contexts by J. Bardeen [Phys. Rev. Letters 1, 399 (1958)] and by J. I. Gittleman, B. Rosenblum, T. Seidel, and A. W. Wicklund [Phys. Rev. 137, A527 (1965)]. The modification had also been discussed and incorrectly dismissed in experiments similar to ours by M. Tinkham [IBM J. Res. Develop. 6, 49 (1962)].

[15]K. Maki, Phys. Rev. Letters 14, 98 (1965).

[16]M. P. Garfunkel, D. Hays, and M. Spalding, Phys. Rev. 183, 501 (1969).

[17]P. W. Anderson, J. Phys. Chem. Solids 11, 26 (1959).

[18]J. Bardeen, L. N. Cooper, and J. R. Schrieffer, Phys. Rev. 108, 1175 (1957).

[19]The details of this model will be discussed in a subsequent paper by M. P. Garfunkel, R. W. Markley, K. Saralkar, and G. Wilkinson (unpublished).

[20]The 1962 He^3 temperature scale: R. H. Sherman, S. G. Sydoriak, and T. R. Roberts, J. Res. Natl. Bur. Std. (U. S.) 68, 579 (1964).

[21]Since the pressure is actually measured by a McLeod gauge at room temperature, thermomolecular pressure corrections are made as described by T. R. Roberts and S. G. Sydoriak [Phys. Rev. 102, 304 (1956)].

[22]Grade 69 aluminum obtained from Cominco Products,

Inc. Spokane, Wash.

[23]This notation is not used universally. Some authors refer to the direction of the static magnetic field with regard to the alternating current, giving the opposite of our notation.

[24]G. Chanin, E. A. Lynton, and B. Serin, Phys. Rev. 114, 719 (1959).

[25]If there is energy-gap anisotropy, the initial onset of absorption measures the smallest or minimum energy gap for that part of the Fermi surface in the plane of the surface of the crystal.

[26]C. Caroli, P. G. deGennes, and J. Matricon, in *Metallic Solid Solutions*, edited by J. Friedel and A. Guinier (Benjamin, New York, 1963).

[27]D. C. Mattis and J. Bardeen, Phys. Rev. 111, 412 (1958).

[28]A. B. Pippard, Proc. Roy. Soc. (London) A191, 385 (1947).

[29]From the BCS theory we have for the critical field, $H_c = (4\pi\rho)^{1/2}\,\Delta = (12\gamma/\pi)^{1/2}\,\Delta/k_B^{-1}$, where ρ is the density of states at the Fermi surface, k_B is the Boltzmann constant, and γ is the coefficient of temperature in the electronic specific heat. Since H_0 is defined by the value of magnetic field at which $pv = \Delta$, and since $\vec{\nabla}\times\vec{H} = (4\pi/c)\vec{J} = (4\pi/c)\,ne\vec{v}$, we get $H_0 = 4\pi ne\lambda\Delta/cp$ for an exponential decrease of field from the surface of the superconductor. Thus $\alpha \equiv H_0/H_c = 2(\pi/3)^{2/3} ek_B \lambda n^{2/3} ch\gamma^{1/2} \approx 1.9$, where we have followed M. A. Biondi and M. P. Garfunkel [Phys. Rev. 116, 862 (1959)], in obtaining the constants; $\lambda = 5.1 \times 10^{-6}$ cm, $n = 1.79 \times 10^{23}$ cm^{-3}, and $\gamma = 1.36 \times 10^{3}$ erg cm^{-2} deg^{-2}.

[30]J. R. Maldonado and J. F. Koch, Phys. Rev. B 1, 1031 (1970).

[31]F. Behroozi and M. P. Garfunkel, Physica 55, 649 (1971).

[32]P. Raynes, Ph.D. thesis (Cambridge University, 1971) (unpublished).

[33]P. Miller, Phys. Rev. 118, 928 (1960).

[34]D. M. Ginsberg, Phys. Rev. 151, 241 (1966).

[35]V. L. Ginzburg and L. D. Landau, Zh. Eksperim. i Teor. Fiz. 20, 1064 (1950).

[36]C. Caroli, Ann. Inst. Henri Poincare 4, 159 (1966).

PHYSICAL REVIEW B VOLUME 7, NUMBER 3 1 FEBRUARY 1973

Effect of Paramagnetic Impurities on Josephson Currents through Junctions with Normal-Metal Barriers

Pramod Kumar

Department of Physics, University of Roorkee, Roorkee, India

(Received 5 June 1972)

The present paper deals with a study of the effect of paramagnetic impurities on zero-bias Josephson currents through junctions with normal-metal barriers at $T = 0\,^{\circ}$K. The ratio of the barrier supercurrent of the impure-SNS (superconductor–normal-metal–superconductor) junction to that of the pure-SNS junction is found to be equal to $1-\zeta$, where ζ is a measure of the impurity concentration. For $\zeta < 1$, the Josephson current is nonzero and decreases with increase of impurity concentration, but in the gapless region ($\omega_g = 0$) when $\zeta \geq 1$, the current is zero for $\zeta = 1$ and then becomes negative for $\zeta > 1$. At $\zeta = 0$, the result is in exact agreement with that of Ishii for the pure case.

I. INTRODUCTION

The supercurrent due to Cooper pair tunneling through superconductor-insulator-superconductor (SIS) junctions has been widely studied both theoretically and experimentally since the discovery of the famous Josephson effect.[1] However, much of the theoretical and experimental work done in this direction pertains to junctions with insulating barriers, and there exist standard techniques, like the Green's-function approach and the tunneling Hamiltonian method, for theoretical study of these junctions. However, not much attention has been given to the theoretical study of the junctions with normal-metal barriers. In the case of such junctions, the usual technique of treating the tunneling Hamiltonian as a small perturbation is not applicable. Instead, one must adopt the Green's-function technique. Ishii[2] has recently applied this technique and determined the one-particle Green's function for pure superconductor–normal-metal–superconductor (SNS) junctions in the thick-barrier limit, choosing a simple model for the junction.[3] He then calculated the dc Josephson current at $T = 0\,^{\circ}$K, using the Green's functions for the superconducting and normal regions.

Ishii does not take into account the effect of impurity scattering in either barrier or superconducting regions. The object of the present study is to investigate the effect of paramagnetic impurities in the barrier and superconducting regions on the Josephson current through junction with normal-metal barriers. For simplicity, we shall restrict ourselves to the case of zero temperature, since all fundamental properties of the Josephson effect are already included in this case. Furthermore, we shall consider the potential difference V between the superconductors to be zero also; i.e., we are